

© 1980 IEEE. Personal use of this material is permitted. However, permission to reprint/republish this material for advertising or promotional purposes or for creating new collective works for resale or redistribution to servers or lists or to reuse any copyrighted component of this work in other works must be obtained from the IEEE.

This material is presented to ensure timely dissemination of scholarly and technical work. Copyright and all rights therein are retained by authors or by other copyright holders. All persons copying this information are expected to adhere to the terms and constraints invoked by each author's copyright. In most cases, these works may not be reposted without the explicit permission of the copyright holder.

JOHN R. ANDERSON AND DAVID KARP

M.I.T. Lincoln Laboratory, Lexington, Massachusetts

ABSTRACT

The MTD (Moving Target Detector) is an automated radar signal and data processing system designed to improve the performance of air surveillance radars in various forms of clutter while providing a low output false alarm rate.

This paper briefly describes the architecture of the MTD processor and presents the results of a field evaluation of the system using the ASR-7 terminal radar at Burlington, Vermont.

1. INTRODUCTION

The goal of the Moving Target Detector development is to produce a fully automated surveillance radar processor capable of providing high detection probability and low-false alarm rate target reports using existing and planned Airport Surveillance Radars and Air Route Surveillance Radars.

An MTD processor has undergone a detailed field evaluation at the Burlington, Vermont terminal ASR-7 radar site. Preliminary results from another ASR-7 installation at the National Aviation Facilities Experimental Center (NAFEC) near Atlantic City are also available. Present plans include the interfacing of an MTD processor to an ASR-8 fully coherent, klystron transmitter terminal radar in the near future.

This paper will briefly describe the architecture of the MTD processing system and present experimental results indicating the performance of the system in operational site environments containing ground, rain and bird clutter.

2. MOVING TARGET DETECTOR2.1 General

A block diagram of the MTD system is shown in Figure 2.1-1. The received IF signal from the radar is smoothly limited to a dynamic range of 51 dB. The IF and COHO signals are then processed with a linear receiver to provide in-phase and quadrature video signals which are sampled with 10-bit A/D converters. This data is stored for the

remainder of an 8-pulse coherent processing interval (CPI) in the input memories of a PMP-2, a parallel programmable signal processor.<sup>[1]</sup> The signal processor performs the doppler filtering and thresholding functions and outputs range, azimuth, doppler and amplitude information for each cell in which threshold crossings are detected. These threshold crossings are then sent to a correlation and interpolation (C & I) processor, where they are first correlated into target reports and then centroided in range and azimuth. These targets are subjected to fixed and adaptive false alarm rejection thresholds to produce target reports. The target reports are finally edited using a scan-to-scan correlator to reduce the output false alarm rate to a typical value of 1 false alarm per 4.7 second scan.

2.2 The ASR-7 Radar

The ASR-7 is a magnetron transmitter terminal radar whose basic parameters are as follows:

Azimuth Beamwidth	1.5°
Pulsewidth	0.833 μs
Instrumented Range	60 nmi
Rotation Rate	12.5 RPM
Wavelength	0.107 M (2.8 GHz)
Transmitter Peak Power	425 kW
Receiver Noise Figure	4.75 dB

When used for MTD operation, the radar is operated in a block-staggered mode with PRFs of 900 and 1100 Hz. The PRF is alternated each CPI to eliminate single PRF blind speeds and increase the likelihood of detecting aircraft with ambiguous doppler velocities in rain clutter. Since the MTD processor, compared to the existing MTI processor, provides more coherent integration gain and improved clutter rejection, it is necessary to increase the stability of the radar system. To do this the ASR-7 stalo has been replaced with a phase-locked crystal oscillator and an AFC servo system has been added to the magnetron. In this configuration the stability (DC-to-residue ratio) of various ASR-7 radars has been measured to be within the range 40 dB to 47 dB single pulse. This instability is believed to be the result of phase noise in the COHO locking and magnetron frequency instabilities. To be of a level such that it would not degrade the performance of the MTD in clutter, a transmitter stability of greater than 50 dB would be required. This level is nominally achieved with the ASR-8 (klystron amplifier) radar system.

\*This work was sponsored by the Federal Aviation Administration. The United States Government assumes no liability for its contents or use thereof.

### 3. MTD SIGNAL PROCESSOR

#### 3.1 General

The basic MTD signal processing structure is a bank of eight 8-pulse FIR filters. One of these filters includes zero doppler velocity and is thresholded using a time averaged ground clutter map. The seven non-zero filters are thresholded using a sliding window range CFAR.

#### 3.2 Doppler Filter Design

The zero velocity filter was designed as a linear phase equiripple low-pass filter<sup>[2]</sup> with the pass band width equal to that part of the doppler spectrum not covered by the seven remaining filters. Stop band side lobes have been constrained to provide good detection performance in rain clutter. The filter coefficients have been quantized to 4 bits plus sign.

The non-zero filters have been designed using the technique of DeLong and Hofstetter<sup>[3]</sup> to approximate the optimum filter for interference composed of 40 dB (single pulse) ground clutter returns with the antenna modulation spectrum, plus a component which is white in doppler except in the vicinity of the target frequency, intended to represent rain clutter. Target frequencies were chosen for seven doppler frequencies spaced across the band. The filters have been further constrained by forcing the realized system function,  $H(z)$ , to be zero at  $z = 1$  when filters are quantized to 5 or 6 bits plus sign. This is to reduce the effect of coefficient quantization on the response to the scanning modulated ground clutter. To increase computation efficiency, filters 5, 6 and 7 have been taken to be the complex conjugates of filters 1, 2 and 3.

#### 3.3 Zero Filter Thresholding

The output of the zero velocity filter is time averaged using a single pole filter for each range-CPI cell (approximately 500,000 cells). Various time constants for this filter have been tested, with the nominal value equal to 16 scans. This filter is thresholded using a threshold multiplier to a designed noise false alarm rate of  $10^{-5}$ .

#### 3.4 Non-zero Filter Thresholding

The non-zero velocity filters are thresholded using a sliding window range CFAR threshold in which the six range cells preceding and the seven range cells following the cell being thresholded and the two adjacent cells are amplitude averaged and multiplied by a threshold to produce a noise false alarm rate of  $10^{-5}$  per filter. This corresponds to a total false alarm rate of about 30 per scan. In the presence of large DC values a fraction (dependent on filter) of the zero filter output is added to the CFAR threshold to control the false alarm data rate.

### 4. POST-DETECTION PROCESSING ALGORITHMS

#### 4.1 General

The post-detection data processing consists of target correlation and interpolation, fixed and adaptive thresholding, and scan-to-scan correlation. All post-processing functions simply filter data to remove false alarms. Output reports consist of actual measured target positions. No smoothing is performed on data that is output to display systems and no track identification is added.

#### 4.2 Fixed-Range and Azimuth-Dependent Thresholding

The purpose of this module is to remove those reports which are due to the presence of automotive traffic or ground clutter whose amplitude is greater than that for which the filter bank is designed. This is accomplished by having a map with high spatial resolution ( $1/4$  nmi by  $2.8^\circ$ ) which is used to store an encoded value indicating the selection of one of two different threshold values with a doppler weighting corresponding to either the scanning modulation residue doppler spectrum, to be used in severe ground clutter areas, or a flat doppler weighting which is used to remove ground traffic. These thresholds are applied to the raw reports before the target correlation process.

#### 4.3 Target Correlation and Interpolation

In this processing module targets are first grouped into clusters on the basis of range and azimuth adjacency. Each cluster is then centroided using a "center of mass" (first moment weighted by amplitude) estimation to produce a centroided range and azimuth. At this point a report "quality" is assigned to the target which is a value extracted from the target parameters representing an estimate of the variance of the azimuth measurement. A "confidence" value is also assigned indicating the likelihood of the report being a false alarm.

#### 4.4 Adaptive Target Thresholding

At many sites the occurrence of targets due to birds or "angels" is a common occurrence. Angel reports have been observed to have a roughly log normal amplitude distribution with a mean cross section of approximately -25 dBSM (square meter). In contrast the population of aircraft targets has an apparent mean cross section (including beam losses) of slightly less than 0 dBSM. Thus there exists with sufficient integration a way to determine if angel false alarms are present in a given target sample. An example of the cross section population of birds and aircraft targets from Burlington, Vermont is given in Figure 4.4-1. As the distributions overlap, it is impossible to precisely determine whether a particular report is due to an aircraft or a bird. Instead we attempt to limit the angel false alarm rate to a fixed maximum value with as little loss in aircraft

detection as possible. The method used to accomplish this is to integrate over a space-doppler area for sufficient time to accurately make an estimate of the angel false alarm rate, and if this exceeds a predefined value (nominally 60 per scan in the entire coverage area) the threshold for that cell is raised. If the rate is significantly less than the acceptable false alarm rate, the threshold is lowered.

Due to the conflict between fast response and sufficient target statistics we have implemented this thresholding as a series of two sequential filters. The first integrates over a relatively long time ( $\sim 200$  sec) using fine spatial cells (16 sq nmi by 3 doppler bins), the second is much faster acting ( $\sim 5$  sec) integrating over the entire coverage space for ranges less than 20 nmi again using 3 doppler bins. The purpose of this organization is to achieve fast response at the onset of false alarms while providing localized attenuation for longer lived phenomena. An example of the performance of this algorithm in heavy angel conditions is given in Figure 4.4-2 using data from NAFEC.

#### 4.5 Scan-to-scan Correlation

The targets which survive the adaptive thresholding process are then input to the scan-to-scan correlator. The scan-to-scan correlator uses tracking algorithms to edit the reports to remove those false alarms which do not have the scan-to-scan position relationship expected of an aircraft target. A significant property of the design of the MTD tracker was the decision not to place a lower limit on the velocity of the tracks. This was done to avoid suppressing the detection of helicopters and small aircraft in head winds. The ability to not enforce this restriction is in the most part provided by the effectiveness of the adaptive thresholding in reducing the angel false alarm rates. To remove stationary false alarms, the output of targets correlated with tracks which have never been greater than 1/4 nmi from the position of track initiation is suppressed.

The processing of this module is relatively straightforward. First input targets are associated with tracks on the basis of a normalized error distance from the track predicted position. Non-unique track-target associations are then resolved and targets correlating with tracks older than 2 scans are output to the display system. The tracks which have been correlated with a target are updated using the target quality to determine the amount of smoothing to be used in the azimuth prediction. Tracks not associated with targets are "coasted" for up to 3 scans (depending on age) and are then dropped. All uncorrelated targets which are not low confidence are retained for use in starting new tracks on the next scan. The current implementation of the MTD tracker uses  $\alpha, \beta$  smoothing ( $\alpha, \beta$  dependent on target quality) in an  $x, y$  coordinate system for track prediction when the track is at ranges less than 6 nmi and a  $\rho, \theta$  coordinate system when the track is outside this range.

## 5. PERFORMANCE EVALUATION RESULTS

### 5.1 Introduction

As of this writing approximately 250 hours of recorded MTD data are available from the Burlington and NAFEC radars containing information on targets of opportunity and planned test flights. The Burlington site is characterized by areas of extremely high amplitude ground clutter, the largest ground clutter returns exceeding 70 dB single-pulse clutter-to-noise at the STC output. Fig. 5.1-1 is a plot of Burlington ground clutter greater than 40 dB C/N. The NAFEC site is not a severe test of ground clutter capability. However, large numbers of angel returns are frequently observed. The NAFEC site is also equipped with a co-rotating DABS monopulse beacon system which provides aircraft altitude information and an independent measurement of aircraft position.

### 5.2 Overall Performance

The MTD has demonstrated reliable automated low false alarm rate performance in a variety of weather and clutter environments. The mean output false alarm rate of the MTD processor is approximately 0.3 per scan with output false alarm rates of above 2 per scan being very rare. Fig. 5.2-1 shows 100 scan (approximately 8 min.) plots of interpolated target reports and the output of the surveillance processor with data from Burlington, Vermont. An isolated plot of results from a one-hour flight test using a Piper Navajo (mean cross section approximately +3 dBsm) is given in Figure 5.2-2. During this test flight the aircraft was detected with an overall probability of 0.94. Approximately 300 scans of the flight are in high clutter areas southwest of the radar. In these areas the detection probability is 0.86. The mid-doppler-band subclutter visibility at Burlington is limited to about 36 dB due to the radar system instability noise (-42 dB single pulse for the Burlington radar) and can be improved with a fully coherent transmitter. Over very large clutter, edge doppler filter (filter 1, 2, 6 and 7) detection is further limited by scanning modulation of ground clutter larger than that for which the filter bank is optimized.

The azimuth accuracy of the NAFEC sensor has been characterized using the DABS beacon system, which has a measured one standard deviation azimuth error of  $.03^\circ$ , as a reference. The MTD azimuth error distribution as shown on Fig. 5.2-3 is comprised of a central normal population with a standard deviation of  $0.10^\circ$  when corrected for quantization effects, and a second smaller component of considerably greater variance which is due to the structured error associated with interpolation processing of low quality targets. The range error population measured this way is essentially normal with a standard deviation of 200 ft. The majority of this error is believed to be due to the variation in the beacon transponder delay. A measurement of the range error using a procedure of a least squares fit of a second order curve to non-manuevering tracks yields a one standard deviation range error of approximately 100 ft.

Throughout the testing, the MTD detection performance in rain has been shown to be superior to that of existing MTI systems. Fig. 5.2-4 shows the detection of an aircraft in rain of 30 dB S/N.

#### 6. CONCLUSION

A long-term demonstration of MTD performance in a difficult FAA field environment has shown that the use of modern signal/data processing techniques does support automation of terminal area surveillance radar systems. The field test results also show that the automated radar combined with a modern beacon system improves the overall sensor surveillance performance.

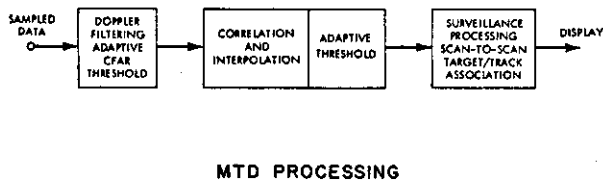


Fig. 2.1-1. MTD Processing Block Diagram

#### REFERENCES

1. C. E. Muehe, "The Parallel Microprogrammed Processor (PMP)," RADAR '77, London, England.
2. L. R. Rabner, J. H. McClellan, T. W. Parks, "FIR Filter Design Using Weighted Tchebyshev Approximation," Proc. of the IEEE (April 1975).
3. D. F. DeLong, Jr. and E. M. Hofstetter, "On the Design of Optimum Radar Waveforms for Clutter Rejection," IEEE Trans. on Information Theory (July 1967).

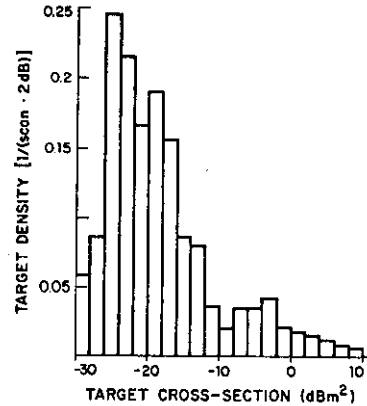


Fig. 4.4-1. Target Apparent Cross-Section Distribution, Burlington, Vermont

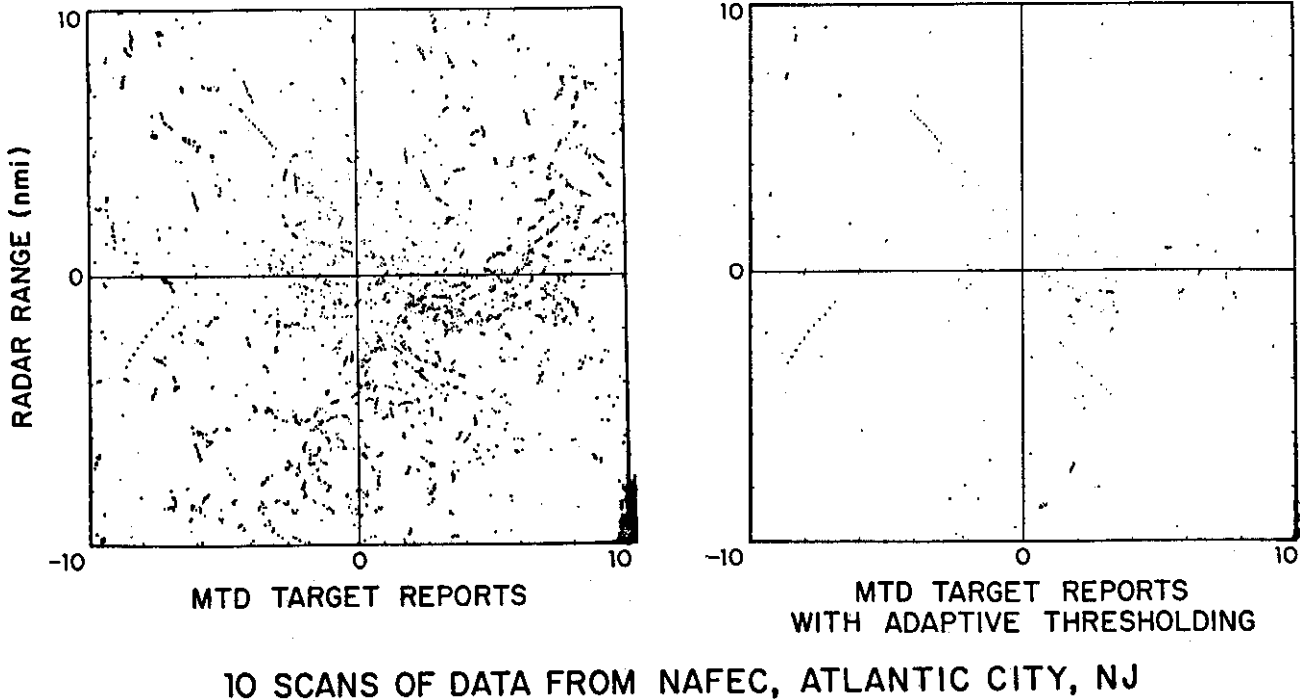
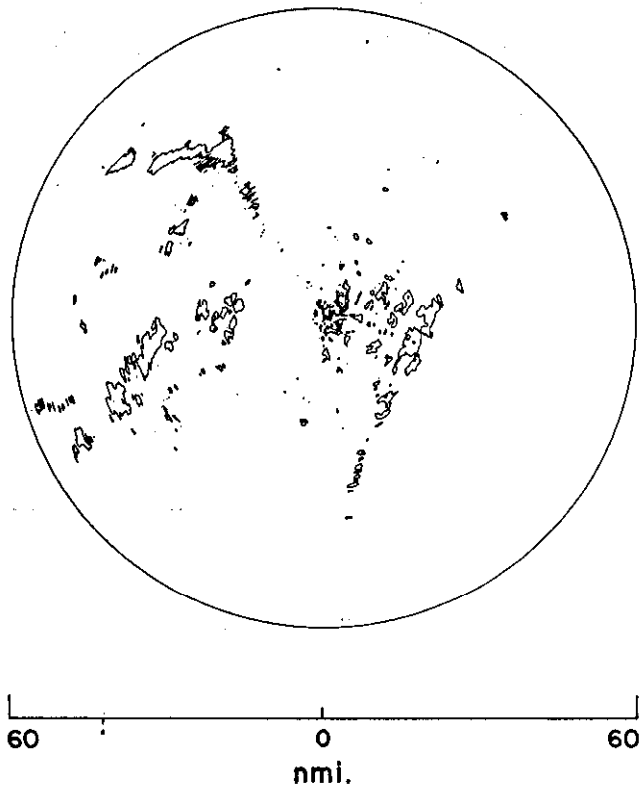


Fig. 4.4-2. Adaptive Thresholding in Heavy Angels



BURLINGTON VT. GROUND CLUTTER (40 dB S/N)

Fig. 5.1-1. Burlington, Vermont Ground Clutter (40 dB S/N)

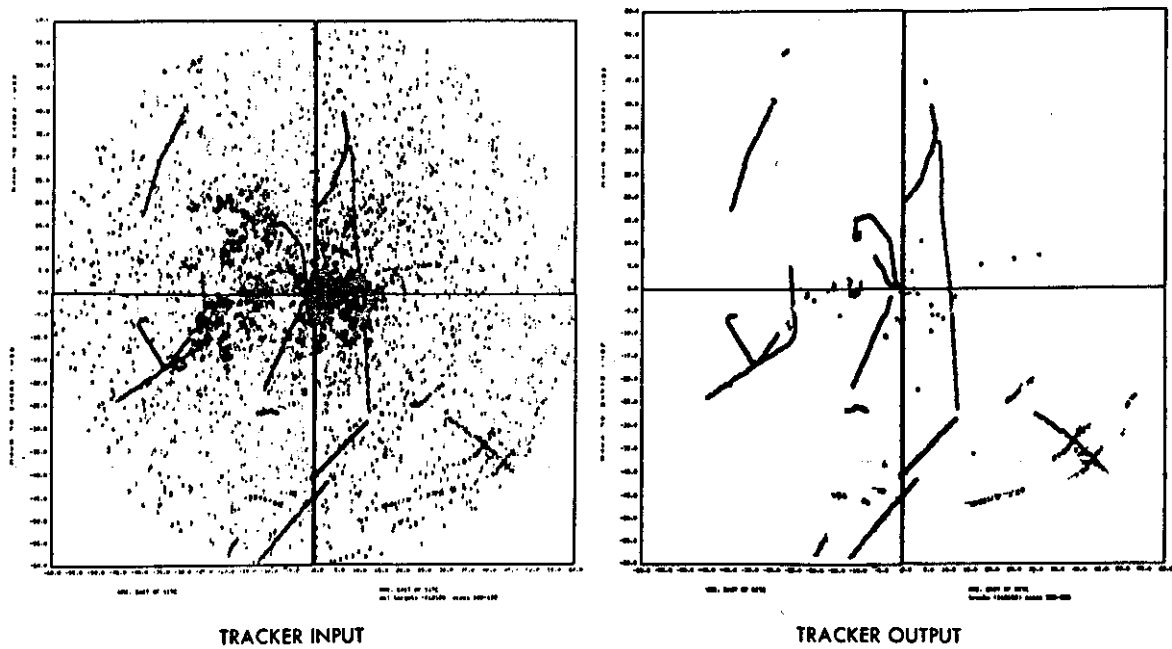


Fig. 5.2-1. MTD Targets and Tracker Output (100 Scans, 60 nmi radius)

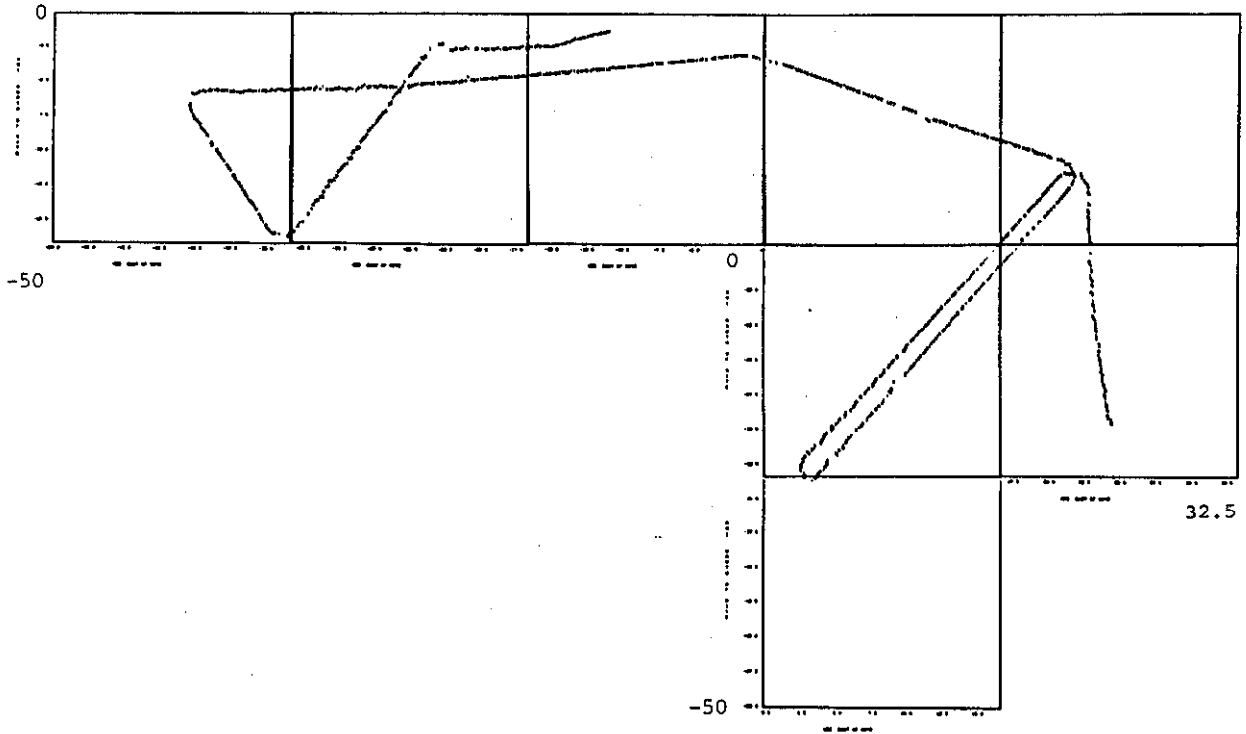


Fig. 5.2-2. Tracker Output for Cessna 172 Test Flight

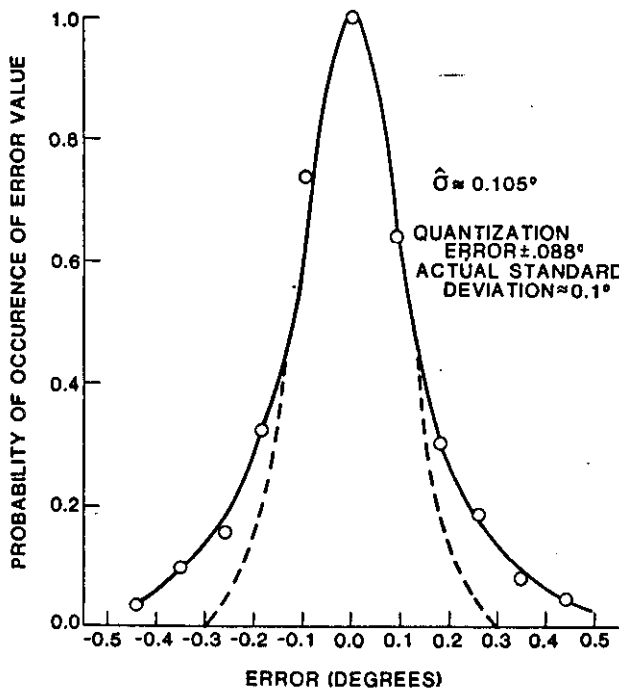
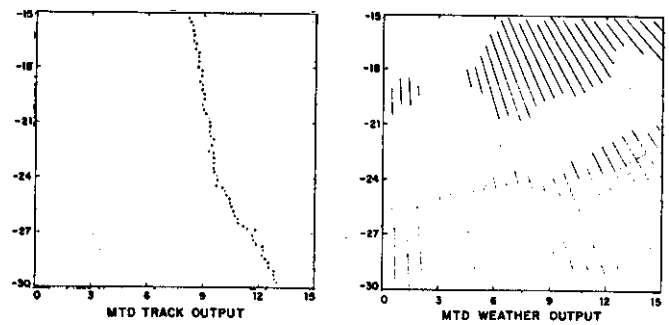


Fig. 5.2-3. MTD Azimuth Error Distribution



MTD PERFORMANCE IN RAIN  
(Shaded Areas 30dBz Rainfall, Cross-Hatched 40dBz)

Fig. 5.2-4. MTD Performance in Rain  
(target of opportunity)